

# Bonding, motional anisotropy, and metal atom dynamics of iron in two ferrocene substituted boron ring compounds

Israel Nowik<sup>a</sup>, Matthias Wagner<sup>b</sup>, Rolfe H. Herber<sup>a,\*</sup>

<sup>a</sup> *Racah Institute of Physics, The Hebrew University of Jerusalem, 91904 Jerusalem, Israel*

<sup>b</sup> *Institut für Anorganische Chemie, Universität Frankfurt, Marie-Curie Strasse 11, D-60439 Frankfurt am Main, Germany*

Received 13 February 2003; received in revised form 21 July 2003; accepted 21 July 2003

## Abstract

Temperature-dependent <sup>57</sup>Fe Mössbauer spectroscopy over the range  $90 \leq T \leq 360$  K has been used to elucidate the hyperfine interactions and dynamical behavior of the iron atom in two ferrocenyl substituted six-membered ring compounds. The root-mean-square amplitude of vibration (rmsav) of the iron atom in ferrocenyl boroxine **I** extracted from the Mössbauer measurements is in good agreement with the average  $U_{ij}$  values observed in X-ray diffraction experiments, but is in less good agreement with the X-ray data reported for ferrocenyl borazine **II**. Moreover, the Mössbauer data lead to the conclusion that with respect to the iron atom motion, the boroxine compound **I** is a softer lattice than **II**. Significant motional anisotropy of the iron atom at 294 K is observed in **I** in agreement with the room temperature X-ray data reported earlier.

© 2003 Published by Elsevier B.V.

**Keywords:** Ferrocenyl borazine; Ferrocenyl boroxine; Mössbauer spectroscopy; Iron atom dynamics

## 1. Introduction

The extensive use of ferrocene-based macromolecular organometallics in the preparation of opto-electronic devices [1–5] and biochemical sensors [6] has emphasized the importance of elucidating the detailed static and dynamic properties of the corresponding precursors in the quest for new and unique materials. In the present study, two six-membered ring compounds, each containing three boron atoms substituted with a ferrocenyl group, have been examined in some detail by using <sup>57</sup>Fe Mössbauer spectroscopy over a wide temperature range. The two compounds critically examined are  $[(\eta^5\text{-C}_5\text{H}_5)\text{Fe}(\eta^5\text{-C}_5\text{H}_4)\text{BO}]_3$  (**I**) [7,8], a boroxine, and  $[(\eta^5\text{-C}_5\text{H}_5)\text{Fe}(\eta^5\text{-C}_5\text{H}_4)\text{BNH}]_3$  (**II**), a borazine first synthesized and described by Kotz and Painter [9], for which an improved synthesis and detailed crystal structure analysis have recently been reported by Wagner and co-workers [8,10].

## 2. Results and discussion

In common with all other diamagnetic ferrocenyl complexes so far examined, the resonance spectra of **I** and **II** consist of a single quadrupole split doublet with well resolved absorption maxima. A typical spectrum of **I** is shown in Fig. 1. The hyperfine parameters, the isomer shift (I.S.) and quadrupole splitting (Q.S.) of **I** and the derived parameters are summarized in Table 1. The I.S. at 90 K is very similar to that of the parent ferrocene [11] and reflects the fact that the *s*-electron density at the iron atom is not sensitive to  $\sigma$ -bond substitution on the Cp ring. In this context it is interesting to note that the I.S. for both **I** and **II** (vide infra) are only ca.  $0.01 \text{ mm s}^{-1}$  smaller than that observed for  $\text{FcB}(\text{OH})_2$ , a monomer, and  $(\text{FcB}=\text{O})_3$  (the latter presumably a cyclic trimer on the basis of extensive mass-spectroscopic data), formed by dehydration of the former at ca. 345 K [12], and the Q.S. values are nearly identical to those observed for the  $\text{FcB}(\text{OH})_2$  and  $(\text{FcB}=\text{O})_3$  compounds. Thus the ring geometry involving the boron atom in **I** and **II** appear to have little effect on the hyperfine parameters observed for the iron atom, while the temperature dependence of the

\* Corresponding author.

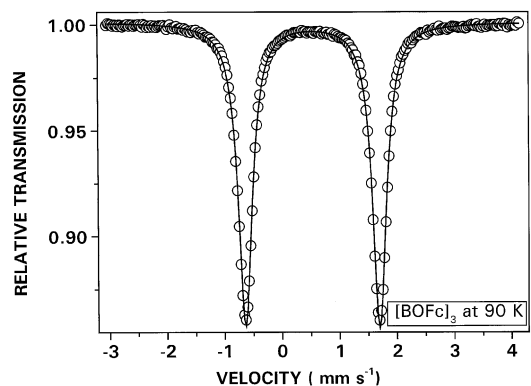


Fig. 1.  $^{57}\text{Fe}$  Mössbauer spectrum of **I** at 90 K. The velocity scale is determined from a metallic iron foil spectrum and the zero point is relative to the centroid of this reference spectrum.

recoil-free fraction ( $-d\ln A/dT$ ) in the high temperature regime (vide infra and Table 1) is significantly smaller for  $\text{FcB}(\text{OH})_2$  than for either **I** or **II**, consistent with molecular weight systematics.

The temperature dependence of the I.S. shows some curvature in the low temperature range (90–230 K) but is well fitted by a linear regression at higher temperatures (230–360 K) with a correlation coefficient of 0.997 for 16 data points. From the slope of this linear regression [ $-(4.94 \pm 0.19) \times 10^{-3} \text{ mm s}^{-1} \text{ K}^{-1}$ ] the effective vibrating mass [13] of the iron atom ( $M_{\text{eff}}$ ) is calculated to be 84 dalton. The difference between this value and the ‘bare’ iron atom mass of 57 dalton reflects the covalency of the metal–ligand  $\sigma$  bond.

The temperature dependence of the area under the resonance curve,  $A(T)$ , which for an optically ‘thin’ absorber scales with the temperature dependence of the recoil-free fraction ( $f$ ), is summarized graphically in Fig. 2. Wagner and co-workers [8] have noted that the boroxine complex exists in two crystallographic modifications, with a phase transition at 283(2) K. The anisotropy of the iron atom motion at room temperature is clearly reflected in the 50 % probability level ellipsoids of vibration shown in the structures, and will be discussed more fully below. The room temperature form (orthorhombic, space group  $Cmc2_1$ ,  $Z = 4$ ) and the low temperature form (154 K, monoclinic, space group

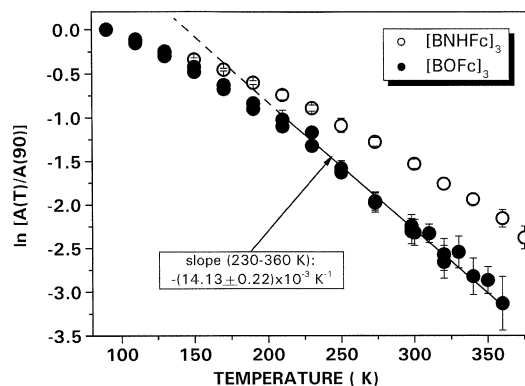


Fig. 2. Temperature dependence of the logarithm of the recoil-free fraction for **I**, full circles, and **II**, open circles. The fit of the data in the high temperature regime for **I** is indicated by the full line in the figure.

$P2_1$ ,  $Z = 2$ ) differ primarily in the relative orientation of the cyclopentadienyl rings of Fe2 (Fig. 1, Ref. [8]) leading to a loss of mirror symmetry in the latter. Thus, it is not surprising that the  $\ln A$  data extracted from the Mössbauer spectra do not show a pronounced discontinuity at the temperature of the phase transition. On the other hand, as has recently been discussed in detail [14], the  $\ln A$  data can be directly compared with the average  $U_{ij}$  values for the iron atom extracted from the crystallographic data. The  $k^2\langle x^2 \rangle$  values are  $1.01 \pm 0.05$  and  $1.32 \pm 0.02(6)$  at 154 K and  $2.49 \pm 0.10$  and  $3.03 \pm 0.04$  at 294 K for the X-ray and Mössbauer data, respectively, in reasonably good agreement with each other. Finally, in this context, it is worth noting that the  $\ln A(T)$  data in the high temperature regime ( $230 \leq T \leq 360 \text{ K}$ ) are well fitted by a linear regression, as shown in Fig. 2. From these data and the temperature dependence of I.S. it is possible to calculate a phenomenological Mössbauer temperature ( $\Theta_M$ ) [13] equal to 81 K, as noted in Table 1. Thus the high-temperature limiting value assumption (i.e. that  $T \geq \Theta_M/2$ ) made in these calculations appears well justified.

Turning next to the borazine complex **II** the Mössbauer parameters are included in the Table 1 summary, from which it is seen that the I.S. and Q.S. of **II** are very similar to those of **I**, as expected. The  $M_{\text{eff}}$  value for the iron atom extracted from the high temperature (230–

Table 1  
Summary of  $^{57}\text{Fe}$  Mössbauer data for the two compounds discussed in the text as well as for two related ferrocenyl boron complexes

	[BOFc] <sub>3</sub>	<i>T</i> range	[BNHFc] <sub>3</sub>	<i>T</i> range	FcB(OH) <sub>2</sub>	[FcB=O] <sub>3</sub>	Units
I.S. (90)	$0.533 \pm 0.001$		$0.529 \pm 0.001$		$0.540 \pm 0.002$	$0.540 \pm 0.002$	$\text{mm s}^{-1}$
Q.S. (90)	$2.337 \pm 0.001$		$2.337 \pm 0.001$		$2.402 \pm 0.002$	$2.310 \pm 0.002$	$\text{mm s}^{-1}$
$-d\text{I.S.}/dT$	$3.68 \pm 0.08$	90–230	$3.70 \pm 0.03$	90–23	$4.18 \pm 0.20$	$4.18 \pm 0.20$	$10^{-4} \text{ mm s}^{-1} \text{ K}^{-1}$
	$4.94 \pm 0.19$	230–360	$5.13 \pm 0.10$	230–375			$10^{-4} \text{ mm s}^{-1} \text{ K}^{-1}$
$-d\ln A/dT$	$8.42 \pm 0.09$	90–230	$6.30 \pm 0.10$	90–230	$5.88 \pm 0.15$	$9.31 \pm 0.14$	$10^{-3} \text{ K}^{-1}$
	$14.13 \pm 0.22$	230–360	$9.65 \pm 0.15$	230–375			$10^{-3} \text{ K}^{-1}$
$M_{\text{eff}}$	84	230–360	81	230–375			daltons
$\Theta_M$	81	230–360	100	230–375			K

375 K) I.S. data is  $82 \pm 1$  dalton in good agreement with the value extracted for **I**. As was true in the case of the boroxine complex, the Q.S. parameter is weakly temperature dependent, decreasing by ca.  $0.01 \text{ mm s}^{-1}$  over the range 90–350 K, presumably due to thermal expansion of the diamagnetic lattice. In fitting these hyperfine data it is necessary to fix the sign of the Q.S. interaction. To effect this assignment, room temperature transmission measurements were carried out with the sample both under ordinary laboratory conditions and in a 3.6–3.7 kOe magnetic field oriented at right angles to the optical axis of the experiment. In both cases in excess of  $15 \times 10^6$  counts per channel were accumulated prior to data reduction. Detailed analysis of the corresponding  $\chi^2$  values showed that the Q.S. parameter in both **I** and **II** is positive, as it is in ferrocene itself [15], and this sign was used in all subsequent data analyses.

The temperature-dependent recoil-free fraction data for **II** from the low temperature regime ( $90 \leq T \leq 230$  K) measurements were analyzed as above and yield a value of  $k^2\langle x^2 \rangle$  at 298 K of 2.13 which is not in especially good agreement with that calculated from the X-ray  $U_{ij}$  data at 294 of 3.09. However, the high temperature regime ( $300 \leq T \leq 375$  K) recoil-free fraction data yield a value for  $k^2\langle x^2 \rangle$  of 2.84, in reasonable agreement with the X-ray  $U_{ij}$  value. Analysis of the Mössbauer recoil-free fraction data show that the root-mean-square amplitude of vibration,  $[\langle x^2 \rangle]^{1/2}$  (rmsav) of the iron atom in the boroxine compound **I** is larger at all temperatures between 90 and 360 K than it is in the borazine complex **II**, in agreement with the higher  $\theta_M$  value in the latter, but in disagreement with the  $U_{ij}$  values extracted from the X-ray diffraction data. The origin of this disagreement is not clear from the presently available data. The rmsav of the iron atom for **I** and **II** over the temperature range  $90 \leq T \leq 360$  K are summarized in Fig. 3, which shows clearly that this parameter is larger for **I** than for **II** over the whole interval. The differences in the rmsav of the iron atom

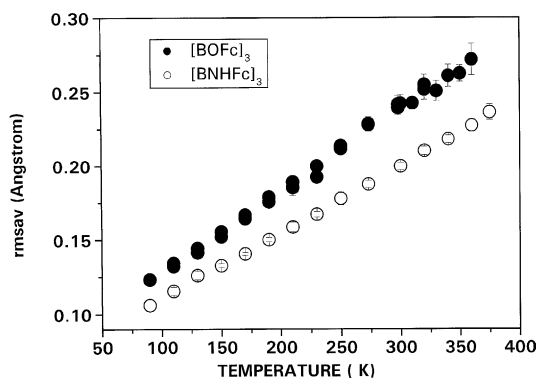


Fig. 3. Temperature dependence of the rmsav of the iron atom in **I** (full circles) and **II** (open circles).

between **I** and **II** range from ca.  $0.02 \text{ \AA}$  at 90 K to ca.  $0.046 \text{ \AA}$  at 360 K. As in the case of **I** the reported phase transition at  $263 \pm 5$  K, which on cooling gives rise to a low temperature form of **II** isomorphous with that in **I**, is not resolvable from either the hyperfine interaction parameters, I.S. and Q.S., or the recoil-free fraction data of the iron atom.

The area ratio,  $R$ , equal to the area of the  $\pi(\pm 3/2 - \pm 1/2)$  gamma transition to that of the  $\sigma(\pm 1/2 - \pm 1/2)$  transition, reflects the anisotropy of the metal atom motion relative to the (local) major symmetry axis which is presumed to be orthogonal to the two Cp rings and includes the metal atom. In this context it should be noted that the positive value of eqQ, established by magnetic field measurements described above, imply that  $\langle x_{\perp}^2 \rangle$  (the mean-square amplitude of vibration perpendicular to the local symmetry axis) is larger than  $\langle x_{\parallel}^2 \rangle$  (the parallel amplitude). This is consistent with similar data reported [14] in other ferrocenyl complexes. Inspection of the crystallographic data of Wagner and co-workers makes it clear that in both compounds at 294 K there is a significant motional anisotropy, with the major axis of the displacement ellipsoid oriented more or less parallel to the Cp ring planes. The temperature dependence of the  $R$  value is summarized in Fig. 4. In consonance with the larger mean-square-amplitude of vibration of the iron atom in **I** compared to that in **II** as noted above, the motional anisotropy, especially above ca. 250 K, is significantly larger in **I** than in **II**. The reported [8] phase transition in **I** at 283 K can be noted in the change of the temperature dependence of  $R$  in the region above ca. 290 K. The first order nature of the crystallographic phase transition is superimposed on the gradual temperature dependence of the vibrational anisotropy, as is evident from the data in Fig. 4. The effect of the crystallographic phase transition in **II** is much less pronounced and cannot be readily resolved from the data.

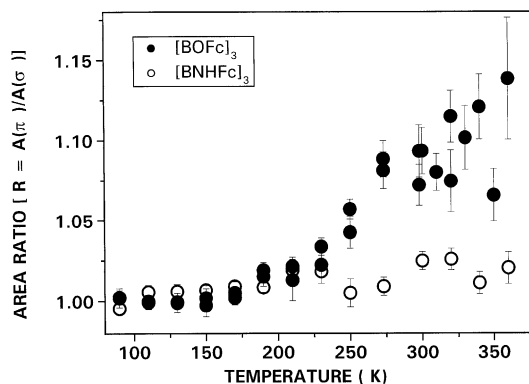


Fig. 4. Temperature dependence of the area ratio for **I** (full circles), and **II** (open circles). The area ratio, in turn, is a reflection of the vibrational anisotropy of the iron atom motion, as discussed in the text.

### 3. Summary

The data extracted from temperature-dependent  $^{57}\text{Fe}$  Mössbauer spectroscopic examination of two ferrocenyl boron complexes have shown that while the hyperfine interaction parameters, I.S. and Q.S., are very similar to those of ferrocene itself, both the vibrational amplitude of the iron atom as well as the anisotropy of this motion can be related to the structural difference in the two complexes. The iron atom rmsav in the ferrocenyl boroxine compound **I** is larger than that observed for the borazine homologue **II** and, at the same time, evidences a larger motional anisotropy (Gol'danskii–Karyagin effect), especially at temperatures in the range  $230 \leq T \leq 360$  K. External magnetic field measurements have shown that the quadrupole hyperfine interaction in both **I** and **II** is positive, as it is in the parent ferrocene.

### 4. Experimental

The samples, were obtained from the Frankfurt group in sealed ampoules. Because of the great similarity in the analytical properties of **I** and **II**, such as the formula weights, the iso-electronic properties of O and NH, the color etc., care was taken to identify the two samples individually. To this end, FTIR spectra of both **I** and **II** were acquired as Nujol mulls. The spectrum of the borazine clearly shows absorbances at 3479, 3440, 3432, and  $3392\text{ cm}^{-1}$  which have been assigned by Kotz and Painter [9] to a medium intensity N–H stretch, as well as an absorbance at  $1475\text{ cm}^{-1}$  assigned to a strong B–N stretch. None of these absorbances are present in the IR spectrum of **I**, and thus the identity of the two samples is clearly confirmed.

Powdered portions of the two compounds were mixed with BN (to optimize random crystallite orientation) and transferred to plastic sample holders in a moisture-free atmosphere, which were then mounted in a variable temperature cryostat, using a Cu-constantan ice-point compensated thermocouple, as described earlier [16].

Spectrometer calibration was effected using a thin  $\alpha$ -iron absorber at room temperature, and all I.S. herein reported are with respect to the centroid of this calibration spectrum. Temperature control and data reduction were effected as described earlier [11,14].

### References

- [1] (a) R.D.A. Hudson, J. Organomet. Chem. 637–639 (2001) 47–69 (and references therein);  
(b) See also T. Mochida, S. Yamazaki, J. Chem. Soc. Dalton Trans. (2002) 3559–3564 (and references therein);  
(c) E. Lindner, R. Zong, K. Eichele, M. Stroeblele, J. Organomet. Chem. 660 (2002) 78–84.
- [2] N.J. Long, Optoelectronic Properties Inorg. Compounds (1999) 107.
- [3] N.J. Long, Angew. Chem. Int. Ed. Engl. 24 (1995) 21.
- [4] Wai-yeung Wong, G. Lu, Ka-Fai Ng, C.K. Wong, Kalto Choi, J. Organomet. Chem. 637–639 (2001) 159–166 (and references therein).
- [5] Z. Yuan, G. Stinger, I.R. Jobe, D. Kreller, K. Scott, L. Koch, N.J. Taylor, T.B. Marder, J. Organomet. Chem. 452 (1993) 115.
- [6] I. Wilner, Science 298 (2002) 2407–2408 (and references therein).
- [7] S.-L. Guo, F. Peters, F. Fabrizi de Biani, J.W. Bats, E. Herdtweck, P. Zanello, M. Wagner, Inorg. Chem. 40 (2001) 4928–4936.
- [8] J.W. Bats, K. Ma, M. Wagner, Acta Crystallogr. C58 (2002) m129–m132.
- [9] J.C. Kotz, W.J. Painter, J. Organomet. Chem. 32 (1971) 231–239.
- [10] K. Ma, H.-W. Lerner, S. Scholz, J.W. Bats, M. Bolte, M. Wagner, J. Organomet. Chem. 664 (2002) 94–105.
- [11] R.H. Herber, I. Nowik, Hyperfine Interact. 136/137 (2001) 699–703.
- [12] E.W. Post, R.G. Cooks, J.C. Kotz, Inorg. Chem. 9 (1970) 1670–1677.
- [13] R.H. Herber, in: R.H. Herber (Ed.), Chemical Mössbauer Spectroscopy, Plenum Press, New York, 1984, pp. 199–216.
- [14] (a) R.H. Herber, I. Nowik, Solid State Sci. 4 (2002) 691–694;  
(b) I. Nowik, R.H. Herber, J. Phys. Chem. Solids 64 (2003) 313–317 (see the correction in *ibid.*, 64 (2003) 1225).
- [15] (a) R.L. Collins, J. Chem. Phys. 42 (1965) 1072–1080;  
(b) B.W. Fitzsimmons, A.R. Hume, J. Chem. Soc. Dalton Trans. (1980) 180–185.
- [16] R.H. Herber, B. Bildstein, P. Denifl, H. Schottenberger, Inorg. Chem. 36 (1997) 3586–3594.